

**Synthesis and Characterization of
Poly[styrene-*block-n*-butyl methacrylate]**

by

Douglas J Harris

Submitted to the Department of Materials Science and Engineering
in partial fulfillment of the requirements for the degree of

Bachelor of Science in Materials Science and Engineering

at the

Massachusetts Institute of Technology

February 1998

© Massachusetts Institute of Technology 1998. All rights reserved.

Author.....
Department of Materials Science and Engineering
January 16, 1998

Certified by.....
Anne M. Mayes
Assistant Professor of Materials Science and Engineering
Thesis Supervisor

Accepted by.....
David K. Roylance
Chairman, Departmental Committee on Undergraduate Students

LIBRARIES

LIBRARIES

Synthesis and Characterization of Poly[styrene-*block-n*-butyl methacrylate]

by

Douglas J Harris

Submitted to the Department of Materials Science and Engineering
on January 16, 1997, in partial fulfillment of the
requirements for the degree of
Bachelor of Science in Materials Science and Engineering

Abstract

Several molecular weights of poly[styrene-*block-n*-butyl methacrylate] block copolymers were anionically synthesized. The polymers were characterized with gel permeation chromatography and nuclear magnetic resonance spectroscopy to determine molecular weight, polydispersity, and composition. Rigorous purification of monomers and solvent resulted in molecular weights between 54K and 210K and polydispersities of 1.1. In addition, the polymers were characterized with small angle neutron scattering to determine their morphologies. A sharp peak at 0.10 nm^{-1} suggests that the 210K diblock copolymer was ordered with a domain spacing of 63 nm. The small angle neutron scattering spectrum of the 54K diblock copolymer had a weak peak at 0.22 nm^{-1} which indicates that the polymer was disordered and has a radius of gyration of approximately 8.5 nm.

Thesis Supervisor: Anne M. Mayes

Title: Assistant Professor of Materials Science and Engineering

Acknowledgments

I would like to thank Prof. Anne M. Mayes for her suggestions, guidance, and support. Philip Soo has helped with anionic synthesis and GPC analysis. I would also like to thank Brandeis University for use of their NMR spectrometer. The SANS spectra were measured by Prof. Mayes and Anne-Valerie Ruzette at the National Institute of Standards and Technology. This research was supported by a grant from Arthur D. Little.

Contents

1 Introduction	7
1.1 Phase Behavior of Block Copolymers	7
1.2 Thermodynamics of LCOT Behavior	8
1.3 Synthesis and characterization of P(S- <i>b</i> - <i>n</i> BMA)	9
2 Literature Survey	10
2.1 Introduction	10
2.2 Anionic Synthesis of P(S- <i>b</i> - <i>n</i> BMA)	10
2.3 Molecular Weight Determination	12
2.4 Free Energy Models of Compressible Macromolecules	14
2.5 Neutron Scattering	16
3 Experimental Apparatus and Procedure	20
4 Experimental Results	22
4.1 Molecular Weight Determination of P(S- <i>b</i> - <i>n</i> BMA)	22
4.2 Determination of dn/dc	23
4.3 Selective Precipitation of Polystyrene Homopolymer	24
4.4 NMR Analysis	24
5 Interpretation of Results.	25
5.1 Polystyrene Homopolymer Contamination	25
5.2 ^1H NMR Analysis	27
5.3 Neutron Scattering.	28
6 Summary and Conclusions.	30
7 Suggestions for Further Work.	31
Bibliography	32
Appendix A	33

List of Figures

1-1. Schematic representation of block copolymer phase diagrams.	8
4-1. Determination of dn/dc for P(S- <i>b</i> - <i>n</i> BMA)	23
5-1 Determination of PS homopolymer in 71K P(S- <i>b</i> - <i>n</i> BMA)	25
5-2 Selective precipitation of 205K P(S- <i>b</i> - <i>n</i> BMA)	26
5-3 NMR spectra of 54K P(S- <i>b</i> - <i>n</i> BMA)	27
5-4 Neutron Scattering of 54K and 210K P(S- <i>b</i> - <i>n</i> BMA)	28

List of Tables

4-1. Composition of synthesized block copolymers. 23

Chapter 1

Introduction

1.1 Phase Behavior of Block Copolymers

Diblock copolymers are linear polymers composed of a block of a repeat unit A, and another block of a different repeat unit, B. Repeat units usually have more energetically favorable interactions with chemically similar repeat units. This generalized rule of "like likes like" often leads to microphase separation into ordered domains of block A and block B. The phenomenon is called microphase separation because the two blocks are chemically attached such that the domains must be small, approximately the radius of gyration of the copolymer. The microphase separation allows block copolymers to combine the properties of two different polymers. Understanding the temperature dependence of the transition between microphase separated and disordered states is important for the processing and application of the copolymers. Block copolymers have found commercial applications as thermoplastic elastomers which contain rigid or glassy blocks and soft, flexible blocks. These polymers are processed at high temperatures to reduce viscosity but physically crosslink by microphase separation when cooled to room temperature. At higher temperatures, the larger number of available configurations of the block copolymer in the homogeneous (disordered) state usually favors random mixing of the blocks and the phase diagram has an

upper critical ordering transition (UCOT). A typical phase diagram is shown in Figure 1-1.

Poly[styrene-*block-n*-butyl methacrylate] (P(S-*b-n*BMA)) is an anomalous block copolymer. For certain molecular weights and compositions, the polymer exhibits UCOT behavior, but at even higher temperature the polymer microphase separates again. This transition at higher temperature has been labeled a lower critical ordering transition (LCOT)¹. Figure 1-1 also shows a schematic phase diagram of P(S-*b-n*BMA).

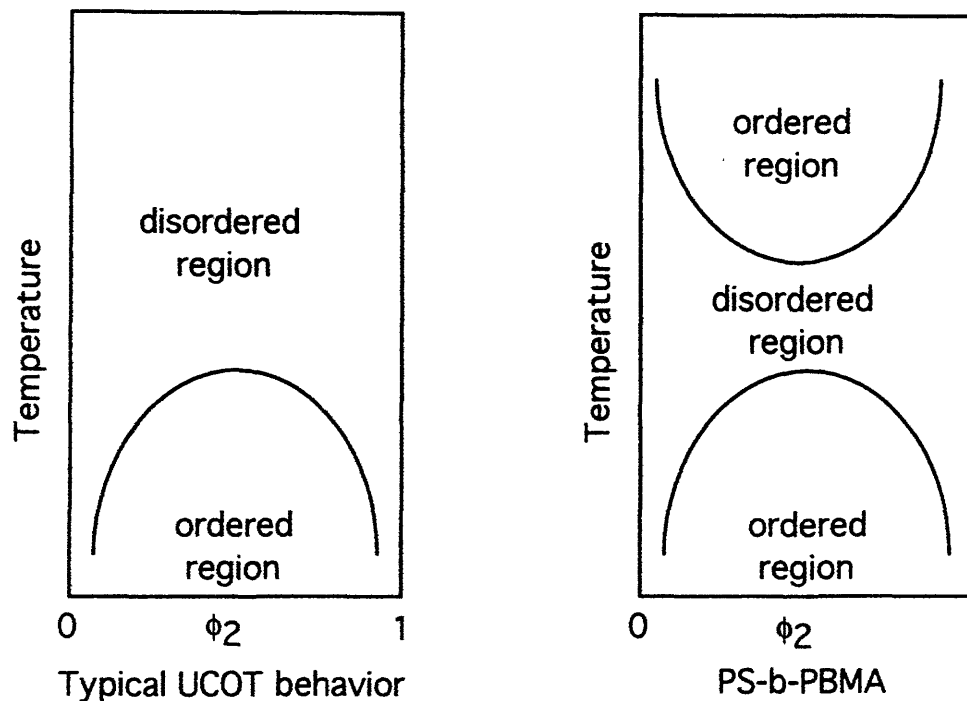


Figure 1-1. Phase diagram of a typical block copolymer (left) and phase diagram of P(S-*b-n*BMA) (right).

1.2 Thermodynamics of LCOT Behavior

The phase diagram is determined by the balance between entropy and enthalpy. The difference between polymers and other materials is the magnitude of the enthalpic term. Each of the many repeat units contributes to the enthalpic driving force which favors microphase separation. The

segmental enthalpic term is characterized by the parameter χ . The total enthalpy of mixing is of the order of χN , where N is the number of statistical segments, related to the degree of polymerization of the polymer. A typical diblock copolymer studied has more than 500 repeat units. The value of χ to overcome the entropy change of mixing for the 68K and 99K molecular weight block copolymers which previously were reported¹ to display LCOT behavior is 0.013-0.019 kT. Near the observed transition, this enthalpy is only ~45 to 78 J/mol of repeat units. Predicting the temperature dependence of this low energy microphase separation is more challenging than predicting the behavior of small molecules, which are insensitive to small variations in energy. Two theories, discussed later, have been postulated on LCOT behavior. More experimental data needs to be obtained to confirm the predictions of these theories.

1.3 Synthesis and characterization of P(S-*b*-*n*BMA)

Synthesis and characterization of P(S-*b*-*n*BMA) systems of varying length and composition are necessary for elucidating the thermodynamic reasons for the anomalous transition. In this study, three block copolymers of different molecular weights were synthesized by anionic polymerization. The polymers were characterized with nuclear magnetic resonance (NMR) and gel permeation chromatography (GPC) to determine the composition, purity, and molecular weights. The morphology of the polymers was determined by small angle neutron scattering (SANS).

Chapter 2

Literature Survey

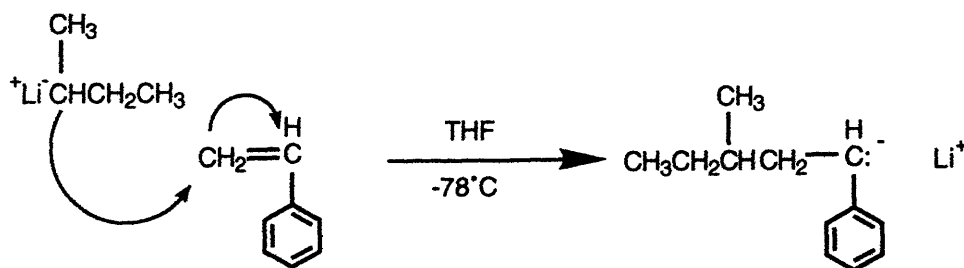
2.1 Introduction

Microphase separation of diblock copolymers with decreasing temperature (UCOT) has been explained by theories that assume incompressibility of the copolymer^{2,3}. The transition has also been extensively studied experimentally^{4,5,6,7,8}. P(S-*b-n*BMA), however, is the first discovered diblock copolymer melt which has LCOT behavior¹. Rheology, x-ray, and neutron scattering were used to experimentally confirm microphase separation on increasing temperature⁹. The rheology measurements show LCOT temperatures ranging from 140°C for a symmetric diblock copolymer with a molecular weight of 87K to 210°C for a 72K symmetric diblock .

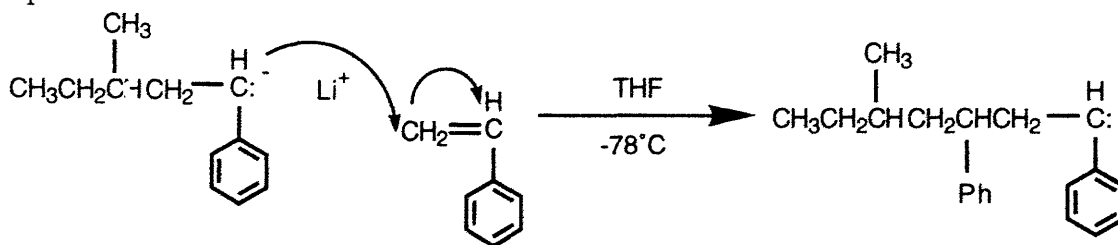
2.2 Anionic Synthesis of P(S-*b-n*BMA)

Anionic synthesis is a convenient method to synthesize the block copolymer. Simple living anionic polymerizations have three steps¹⁰. The three steps for polymerizing styrene are shown below.

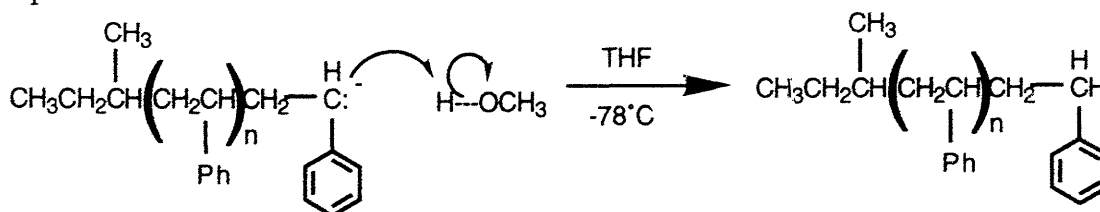
1: Initiation. An extremely strong nucleophile attacks the double bond of a monomer:



2: Propagation. Nucleophilic attack by the living polymer adds additional repeat units to the chain:



3: Termination. Abstraction of a proton from a relatively acidic compound stops the chain reaction:



In a "living" anionic polymerization, the propagating species is stable. The THF must not contain protonic compounds such as water or alcohols, and the atmosphere must be inert. Electron acceptors such as oxygen can terminate the reaction. Typically, the temperature is cold to prevent side reactions which may slowly terminate the polymerization.

The control of molecular weight is a major benefit of living polymerizations. If all of the initiator reacts with the monomer and the polymerization is living, the degree of polymerization \bar{X}_n can be calculated by equation 2.1:

$$\bar{X}_n = \frac{[M]}{[I]} \quad (2.1)$$

The molecular weight of the polymer can thus be controlled by varying the concentrations of initiator [I] and monomer [M].

In addition to controlling molecular weight, anionic polymerization has the potential to produce polymers of low polydispersity. The initiation

step by the strong nucleophile is usually fast compared to propagation. All chains after termination should have approximately the same molecular weight. If mixing is efficient and side reactions do not occur, the size distribution can be calculated by the Poisson distribution¹¹. Equation 2.2 can be used to calculate the polydispersity under these ideal conditions:

$$\frac{\bar{X}_w}{\bar{X}_n} = 1 + \frac{\bar{X}_n}{(\bar{X}_n + 1)^2} \approx 1 + \frac{1}{\bar{X}_n} \quad (2.2)$$

Polymers with a degree of polymerization of 1000 should have a polydispersity of 1.001. Side reactions and mass transport limit the polydispersity of real polymers. Typical living polymerizations have PDI's less than 1.1.

Both poly(*n*-butyl methacrylate)¹² and poly(styrene)¹³ have been synthesized by anionic polymerization as well as block copolymers of these materials¹. Polystyrene is frequently synthesized by the simple nucleophilic attack of *sec*-butyllithium to styrene in cold THF. Poly(*n*-butyl methacrylate) polymerizes by base catalyzed Michael reactions of the α,β -unsaturated carbonyls¹². A strong nucleophilic initiator such as butyl lithium will attack the ester instead of initiating the monomer. A more hindered initiator such as diphenyl methyllithium must be used.

2.3 Molecular Weight Determination

A powerful tool for determining the molecular weight distributions of synthesized polymers is gel permeation chromatography (GPC) with both refractive index and light scattering detectors. GPC forces a dilute polymer solution to flow through a column containing a porous gel¹⁴. Small polymers can flow through the pores of the gel. Larger polymer chains are excluded from the gel and have a shorter path before reaching a detector. The chromatogram shows the highest molecular weight polymer first exiting the

column. By calibrating the column with a set of molecular weight standards, the molecular weight of an unknown can be determined.

A refractometer measures the difference in refractive index when the polymer chains flow through the detector. The change in refractive index is proportional to the concentration of repeat units in the solvent. This detector is very accurate and can detect small concentrations of eluted polymer.

Light scattering, although not as sensitive as refractive index, provides another mechanism of detecting polymers. The scattering intensity of a monochromatic red laser beam is related to the molecular weight and the concentration of the eluted polymer. A combination of refractive index and light scattering allows determination of the molecular weight distributions of synthesized polymers.

Diblock copolymers are more difficult to analyze than homopolymers. Each type of repeat unit has a different refractive index. A polydisperse block copolymer will have chains with different molecular weights and different compositions. A single value of the change of refractive index with polymer concentration (dn/dc) is not possible for the various compositions. A more accurate method of determining the molecular weight of diblock copolymers is a combination of GPC and NMR spectroscopy. A sample of the living first block can be removed and precipitated before the addition of the second monomer to the living polymerization. The molecular weight of this block can be characterized with GPC. The composition of the block copolymer after polymerization of the second monomer can be determined from the ^1H NMR spectrum. The two hydrogens near the ester group of poly(*n*-butyl methacrylate) will have a resonance near 4 ppm while the aromatic hydrogens of poly(styrene) will have a chemical shift near 7 ppm. The areas of the two peaks will be proportional to composition. The average molecular

weight of the diblock copolymer will be equal to the molecular weight of the first block divided by the relative weight fraction of that block in the copolymer.

2.4 Free Energy Models of Compressible Macromolecules

The original derivations of the thermodynamics of ordering transitions in diblock copolymers and polymer blends assume that the polymer melts are incompressible. Several later models incorporate compressibility effects in predicting phase diagrams. These models are based on the metastability condition for a binary mixture: the second concentration derivative of the molar Gibb's free energy at constant pressure must be positive. The effects of compressibility can be incorporated into this stability condition:

$$g_{xx} = (\partial^2 g / \partial x^2)_V - v\beta(\partial^2 g / \partial x \partial v)^2 > 0 \quad (2.3)$$

where β is the isothermal compressibility:

$$\beta = -1/v(\partial v / \partial P)_{T,x} \quad (2.4)$$

which is a positive value. The addition of the second term in Equation 2.3 generally favors the ordered state. As temperature increases, the compressibility effects become larger and LCOT behavior results. Many theories have attempted to quantify the temperature and pressure dependence of the second term.

The Flory, Orwoll and Vrij model¹⁵ is one of the early equation of state models used to quantify compressibility effects. This model treats monomer units as hard sphere repulsive potentials surrounded by soft attractive potentials. The characteristic volume of the hard sphere and the attractive potential are characterized by three parameters, the characteristic volume, pressure, and temperature, v^* , P^* , and T^* . Increasing temperature or decreasing the pressure increases the average distance between the polymer

chains. The increase in volume also increases the entropy of the polymer. Although this entropic effect is usually negligible for small molecules, the large number of monomer repeat units in a macromolecule results in a significant driving force per chain for phase separation or ordering of block copolymers. Differences in the soft attractive potentials for the two blocks of a copolymer can lead to LCOT behavior.

Another common model known as the "lattice fluid" model was developed by Sanchez and Lacombe.¹⁶ In this model the polymer material consists of 2 components: polymer chains and holes. The polymer chains are not limited in their conformations to perfectly fill space. The holes decrease the restrictions on polymer packing and therefore increase entropy. The lattice fluid model can predict LCOT behavior in polymer blends and diblock copolymers if the relative densities in the disordered and ordered states are different. In the ordered state, each block has a different density which minimizes the free energy. In the disordered state, however, both types of repeat units experience an average hole concentration. As the temperature increases, the different coefficients of thermal expansion of the two blocks increases the magnitude of the compressibility term of Equation 2.3. The lattice fluid model has been successful in reproducing observed phase diagrams such as the lower critical solution temperature of poly(isobutylene) in 11 hydrocarbon solvents¹⁷, although the predicted transition temperatures were typically 40°C lower than the observed transition. Sanchez also applied the model to the phase behavior of blends of perdeuterated polystyrene P(d-S) and poly(vinyl methyl ether) (P(VME)) which exhibit LCST behavior¹⁸. Although the experimental spinodal temperatures obtained by SANS are similar to the calculated temperature, the model is not fully satisfactory

because the compositional dependence of the interaction parameter is not correctly predicted.

In another study, SANS measurements were performed on blends of P(d-S)/P(VME) and P(d-S)/P(*n*BMA) under pressure¹⁹. The results show that pressure enhances miscibility for both blends. Only one composition of the P(d-S)/P(*n*-BMA) was studied with SANS but the χ parameter was obtained from extrapolating the data to an infinite wavelength and the calculated value of χ monotonically increases with pressures up to 80 MPa. An important caveat is that the authors used an incompressible model to calculate χ and the results must be cautiously interpreted.

2.5 Neutron Scattering

The wave-like nature of high energy neutrons allows analysis of a material's structure with a theoretical approach analogous to light or x-ray scattering²⁰. The wavelength of a neutron is based on its kinetic energy:

$$\lambda=(h^2/2mE)^{1/2} \quad (2.11)$$

where h is the Planck constant, m is the mass of a neutron, and E is the kinetic energy. The kinetic energy of the neutron can be reduced from the high energy state initially generated by nuclear fission by passing the neutron beam through a cold material such as liquid hydrogen²¹. The kinetic energy of the neutrons is reduced to $3/2 kT$ and the lower energy of these cold neutrons increases the wavelength. The wavelength of the neutron beam can be precisely controlled by Bragg diffraction from an ideal crystal. The 'scattering vector' q , is defined as:

$$q=k_f-k_i \quad (2.12)$$

where \mathbf{k}_f and \mathbf{k}_i are the wave vectors of the incident and scattered waves. The magnitude of \mathbf{q} can be related to the Bragg scattering angle θ_B (the angle between the scattered beam and the lattice planes) by:

$$|q| = \frac{4\pi}{\lambda} \sin \theta_B \quad (2.13)$$

Unlike x-ray scattering where the interaction of the wave and electrons in the material results in the scattered signal, neutron scattering is based on the interaction of the neutrons and the nucleus of atoms. The scattering cross sections of atoms are isotope dependent in neutron scattering. Polymers containing low atomic number elements such as carbon and hydrogen can strongly scatter the neutron beam.

Neutron scattering is useful in the determination of periodicity of micro-phase separated block copolymers. The condition for coherent scattering from a periodic structure is given by Bragg's law:

$$n\lambda = 2d \sin \theta_B \quad (2.14)$$

Disordered polymer blends do not have Bragg diffraction peaks. A method for predicting the observed scattering spectra called the random phase approximation (RPA) was developed by de Gennes²². The classical RPA theory assumes incompressibility and derives the q dependence of scattering intensity by determining the static structure factor $S(\mathbf{q})$. This structure factor is the Fourier transform of the monomer density-density correlation function. Fluctuations in monomer concentrations at a length scale of $1/q$ will cause scattering of neutrons at corresponding values of θ .

The RPA method was applied to incompressible melts of A-B diblock copolymers by Leibler². The free energy of the fluctuations in monomer concentration was calculated using the molecular weight of the polymer and the χ parameter. The most probable concentration fluctuation, the value of q which maximizes $S(\mathbf{q})$, corresponds to the peak observed in the scattering

spectra. In mixtures of two homopolymers, the value of $S(q)$ is maximum at $q=0$ which corresponds to fluctuations of infinite wavelength. However, for diblock copolymers, the connectivity of the two blocks leads to correlation of similar repeat units even in the disordered state. The position of the scattering peak for a disordered diblock copolymer is dependent on molecular weight and composition. For a disordered symmetric diblock copolymer, de la Cruz and Sanchez²³ calculated that the scattering peak for block copolymers with a fraction, f , of A monomers in the copolymer should occur at:

$$q^* = R_g^{-1} \left[\frac{3}{f(1-f)} \right]^{1/4} \quad (2.15)$$

even for systems with $\chi=0$. For symmetric diblocks, this corresponds to a maximum at $1.86R_g^{-1}$. The magnitude of this peak increases with increasing χ and diverges at the spinodal.

Compressibility effects, an important explanation for LCOT behavior, were incorporated into the RPA theory by Dudowicz and Freed,^{24, 25, 26, 27} Bidkar and Sanchez,²⁸ and Yeung et. al.²⁹ Dudowicz and Freed used equation of state models to explain the effective Flory interaction parameter, χ_{eff} . Using the compressible RPA model, the value of χ_{eff} was calculated from scattering spectra of polymer blends including P(d-S)/P(S) and P(d-S)/P(VME). Incorporation of compressibility was necessary to explain the experimental scattering behaviors of the blends. The theoretical models, however, did not provide good quantitative predictions of the experimental SANS data.

Bidkar and Sanchez provided a more thorough analysis of small angle neutron scattering from compressible polymer blends. They used a modified form of the RPA theory to calculate the scattering from a multicomponent compressible polymer blend. The new compressible RPA formula predicts that the intensity at $q=0$ cannot be directly related to χ . If the incompressible

RPA formula was applied to blends with large compressibilities, the radii of gyration can be typically overestimated by 10 or 20% and the value of χ will appear to be dependent both on concentration and on molecular weight.

Also combining RPA and equation of state theories, Yeung et. al. predicted the scattering from diblock copolymers. The free energy of a diblock copolymer was expressed as a function of the order parameters, $\psi_i(r)$. The coefficients of this Landau expansion was calculated by means of the RPA theory. Two characteristic interaction parameters, Δ and Σ , were defined to predict the phase behavior of diblock copolymers. The parameter Σ corresponds to the inverse of the T^* of the equation of state model and is defined as:

$$\Sigma = -[f^2\chi_{AA} + (1-f)^2\chi_{BB} + 2f(1-f)\chi_{AB} - 2f\chi_{SA} - 2(1-f)\chi_{SB}] \quad (2.16)$$

where f is the fraction of segments in block A and χ_{ij} is segmental enthalpic energy between components i and j . In the compressible models, the solvent, S, is the hole component and therefore χ_{SA} and χ_{SB} will be zero. The other interaction parameter, Δ is defined as:

$$\Delta = (1-2f)\chi_{AB} + f\chi_{AA} - (1-f)\chi_{BB} - \chi_{SA} + \chi_{SB} \quad (2.17)$$

The RPA calculations predict that diblock copolymer will have both a UCOT and a LCOT if the value of $N(\Delta/\Sigma)^2 = 60$. If the value is much less than 60, only a UCOT will be observed and if the value is much greater than 60, the polymer will be ordered at low and high temperatures without a disordering transition in between. This theory was applied to P(d-S-b-nBMA) and the results were qualitatively in agreement with the observed ordering behavior.

Chapter 3

Experimental Apparatus and Procedure

THF was refluxed overnight over Na and benzophenone until the solution turned dark purple, indicating complete reaction with oxygen and water. The THF was then distilled into an oven-dried and nitrogen filled 500 mL Strauss flask. Approximately 400 mL of THF was distilled for each synthesis. The flask was then cooled to $-78\text{ }^{\circ}\text{C}$ in a dry ice/acetone bath. During cooling, a positive pressure of nitrogen was maintained. Styrene monomer (99+%) was twice vacuum distilled from lithium aluminum hydride and 20 mL (18.2 g) was injected through the septum of the Strauss flask. 400 μL of *Sec*-butyllithium (1.3M solution in cyclohexane) was then injected into the flask. The orange solution was stirred for 30 minutes and maintained at dry ice temperature. A fraction of the polymer was removed to characterize the styrene block of the copolymer. Diphenylethylene was vacuum distilled from calcium hydride and 0.2 mL (0.0011 mmoles) was injected into the living polymer solution. The color immediately changed to a dark red. Butyl methacrylate was twice vacuum distilled from calcium hydride and 20.2 mL (18.2 g) was injected into the flask. The solution immediately changed to a faint green color. The solution was stirred for half an hour. The living polymerization was terminated by addition of methanol. The solution was precipitated in a large volume of methanol and filtered with a large Buchner funnel. The white polymer was dried overnight on top of a warm oven to evaporate remaining solvent. Typical yields of polymer were only 90% due to losses during precipitation and filtration.

A Waters GPC powered by a 590 HPLC pump with two HR4 columns, a Waters 410 refractometer, and a Wyatt light scattering detector was used to determine the molecular weight and polydispersity of both the styrene homopolymer and the diblock. The columns are effective for molecular weights between 5000 and 500,000 g/mol. The precipitated polymers were dissolved in HPLC grade tetrahydrofuran. The concentration was approximately 4 mg/mL. The solutions were filtered with a 0.5 micron Teflon filter. Then, 75 μ L were injected into the sample loop of the GPC machine. The flow rate of the machine was 1 mL/minute. Light scattering and refractive index detectors recorded the output of the columns. The light scattering detector was calibrated with diblock solutions containing 0, 0.246, 0.491, 0.737, 0.982, and 1.23 mg polymer / mL of THF.

The GPC chromatograms showed a polystyrene homopolymer impurity in the block copolymer. Selective precipitation was used to remove some homopolymer impurity from the block copolymer. A solution was prepared of 1 wt% polymer dissolved in benzene. Methanol was added until the solution became cloudy (approximately 35 wt% methanol). The solution was allowed to equilibrate for 48 hours. No precipitate settled to the bottom of the flask. This suggests that the poly(styrene) homopolymer was trapped inside of micelles because pure poly(styrene) solutions quickly precipitate when the methanol concentration is raised above 35%. Additional aliquots of methanol were added and the solution was allowed to equilibrate for 48 hours after each aliquot. At approximately 60 wt% methanol, some precipitate had settled to the bottom after 48 hours. The precipitate was filtered and analyzed with GPC. The remaining solution was precipitated and also analyzed with GPC.

Chapter 4

Experimental Results

4.1 Molecular Weight Determination of P(S-*b*-*n*BMA)

The GPC chromatograms of the three synthesized block copolymers are shown in Figures A-1, A-2, and A-3. The GPC of the polystyrene block of the polymers shown in Figures A-1 and A-3 were recorded on an older GPC instrument with poor columns and an accurate molecular weight was not obtained. The polystyrene block of the third copolymer was recorded and the chromatograms are overlaid in Figure A-2. The ^1H spectra for sample A-1 is shown in Figure A-7. Table 5-1 summarizes the molecular weights of the synthesized block copolymers. The molecular weights of the styrene blocks for samples 1 and 3 were not determined by GPC and were calculated by the composition determined by the ^1H NMR spectra and GPC results of the diblock copolymers. The results of the GPC chromatograms for diblock copolymers are relatively inaccurate because dn/dc changes with molecular weight and standards are not available to calibrate diblock copolymer molecular weights. Comparison of a copolymer which was analyzed both by GPC of the diblock copolymer and the combination of GPC of the styrene block and NMR composition analysis shows that the GPC calculation alone is 15% lower than the combination of GPC and NMR. The desired molecular weights of all three block copolymers was 70K. A significant fraction of the initiator was neutralized by impurities in sample 3.

Table 4-1. Composition of synthesized block copolymers.

Sample	PS M_n	PS M_w	P(S- <i>b</i> - <i>n</i> BMA) M_n	P(S- <i>b</i> - <i>n</i> BMA) M_w	PDI	wt% PS
1	26.8K		48.7K	53.7K	1.10	55%
2	27.3K	30.6K	66.2K	71.1K	1.07	41%
3	98.9K		184.8K	210.4K	1.14	53%

4.2 Determination of dn/dc

The dn/dc value of the diblock copolymers was determined by measuring the refractive index of solutions of known concentrations. Figure A-4 shows the experimental results. Figure 4-1 shows the change in refractive index with increasing polymer concentration. The slope of the best fit line is 0.103. The y-intercept is not zero because the THF in the solutions had a slightly different refractive index compared to the THF in the GPC.

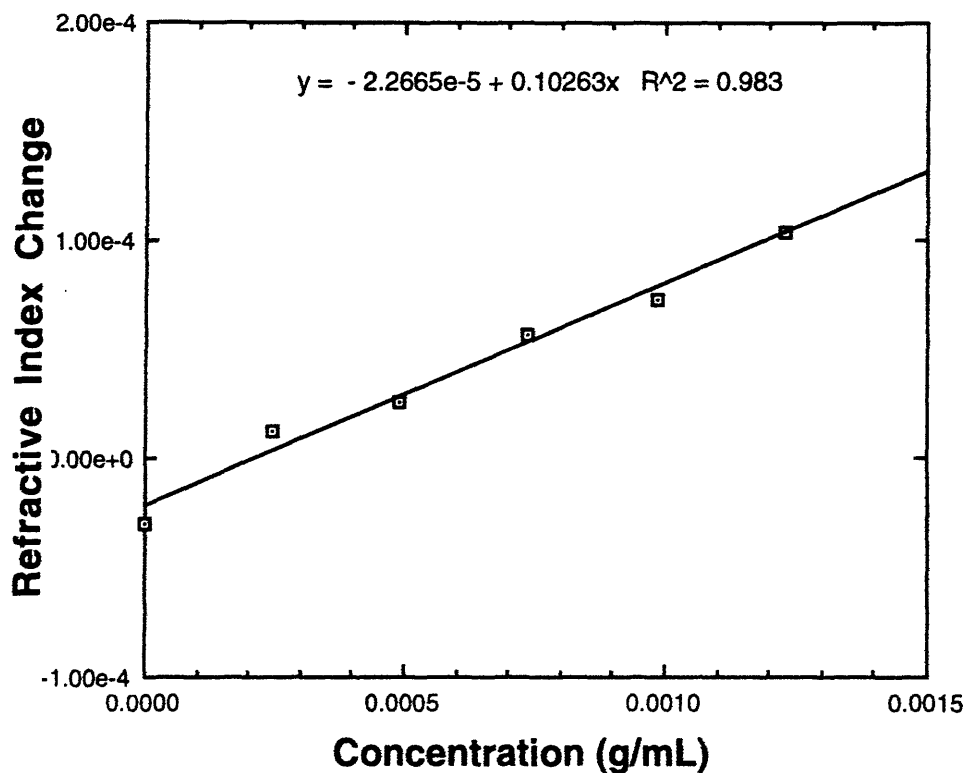


Figure 4-1. Determination of dn/dc for P(S-*b*-*n*BMA)

4.3 Selective Precipitation of Polystyrene Homopolymer

Sample 2 (71K) and sample 3 (210K) were used for the selective precipitation experiments. The mass of the precipitated fraction in sample 2 was 70% of the initial dissolved polymer. The precipitate in sample 3 was only 5% of the initial dissolved polymer. The GPC chromatograms of the precipitated and remaining fractions of 71K diblock copolymer are shown in Figure A-5. The results for the 210K copolymer are shown in Figure 5-2.

4.4 NMR Analysis

The ^1H spectra of the 54K copolymer was analyzed with a 500 MHz Bruker spectrometer at Brandeis University. The 210K sample was analyzed with a 300 MHz Varian spectrometer at MIT. Approximately 20 milligrams of each polymer were dissolved in 1 mL CDCl_3 and pipetted into a 5 mm diameter NMR tube. The probe temperature was maintained at 300 K. A high ratio of signal to noise was obtained after 8 scans with a delay time of 3 seconds between each scan. The spectrum of the 54K copolymer is shown in Figure 5-3.

Chapter 5

Interpretation of Results

5.1 Polystyrene Homopolymer Contamination

The gel permeation chromatograms suggest that some polystyrene homopolymer contaminates the diblock copolymer. The amount of impurity in the 71K diblock was quantified by subtracting the chromatogram of the polystyrene homopolymer from the chromatogram of the diblock copolymer. The change of refractive index for each chromatogram was normalized by dividing by the mass of injected polymer and the value of dn/dc (0.193 for polystyrene and 0.103 for the diblock copolymer). Figure 5-1 shows the molecular weight distributions of the 71K diblock after subtracting different fractions of the polystyrene homopolymer chromatograms. The curve that has the best shape contains $10 \pm 2\%$ polystyrene homopolymer.

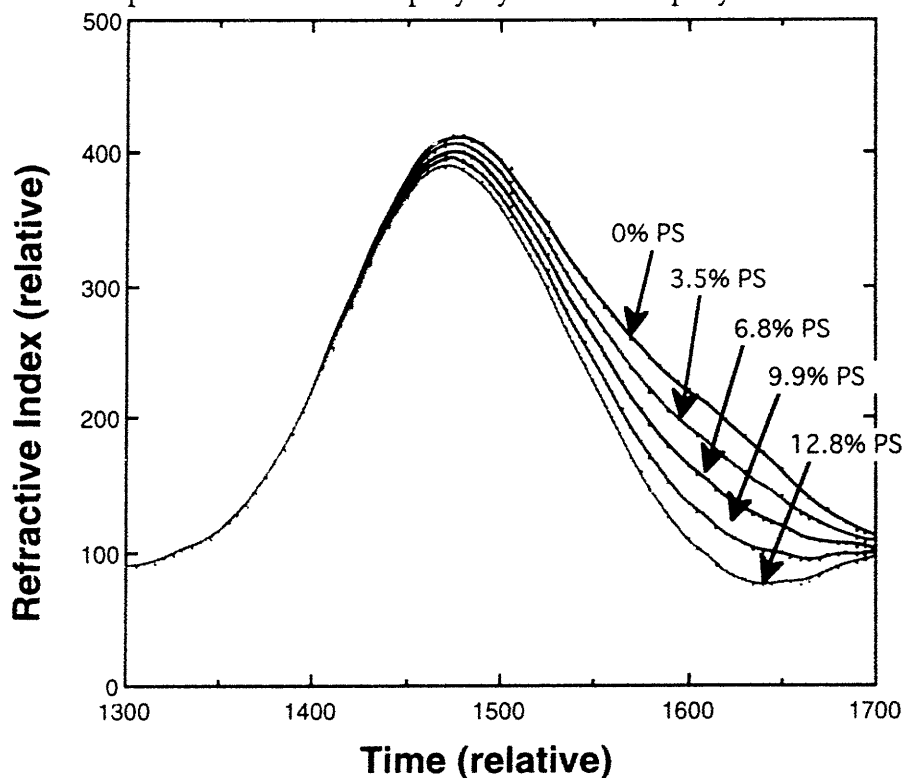


Figure 5-1. Determination of polystyrene homopolymer in 71K P(S-b-nBMA).

The selective precipitation of the 71K block copolymer showed little improvement in purity. The polystyrene impurity did not first precipitate. The GPC chromatograms in Figure A-6 still have a broad right shoulder corresponding to polystyrene impurity. The precipitation of the 210K P(S-*b*-*n*BMA) was more successful. The 5% precipitate was high molecular weight polystyrene homopolymer. Figure 5-2 shows that the remaining polymer had a smaller low molecular weight shoulder and most of the higher molecular weight impurity had precipitated. Because the dn/dc of poly(styrene) is approximately twice as large as the dn/dc value of the diblock, the residual shoulder height is larger than the actual mass of contaminating homopolymer. The residual homopolymer appears to be less than 5% of the diblock copolymer.

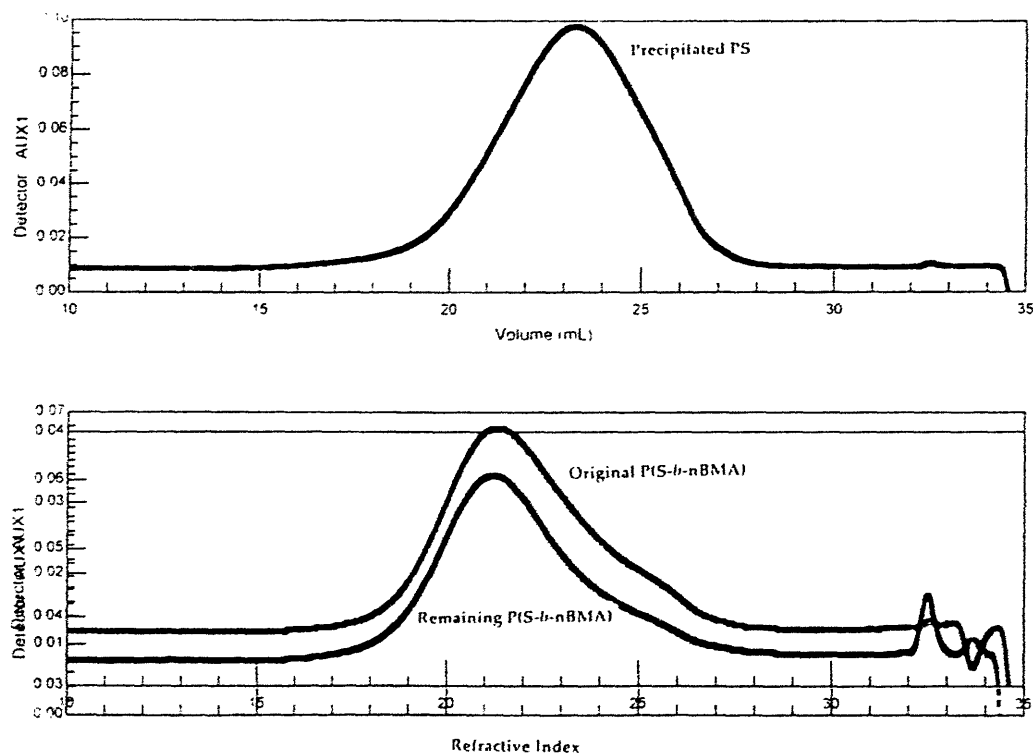


Figure 5-2 Selective precipitation of 205K P(S-*b*-*n*BMA).
Precipitated Material: $M_n=80K$, $M_w=94K$

5.2 ¹H NMR Analysis

Figure 5-3 shows the ¹H NMR spectra of the 54K diblock copolymer dissolved in CDCl₃. The composition of each copolymer was determined by the relative integrals of peaks. The two peaks in the region near 7 ppm correspond to the five phenyl hydrogens of styrene. The peak slightly above 4 ppm corresponds to the -OCH₂- group of *n*-butyl methacrylate.

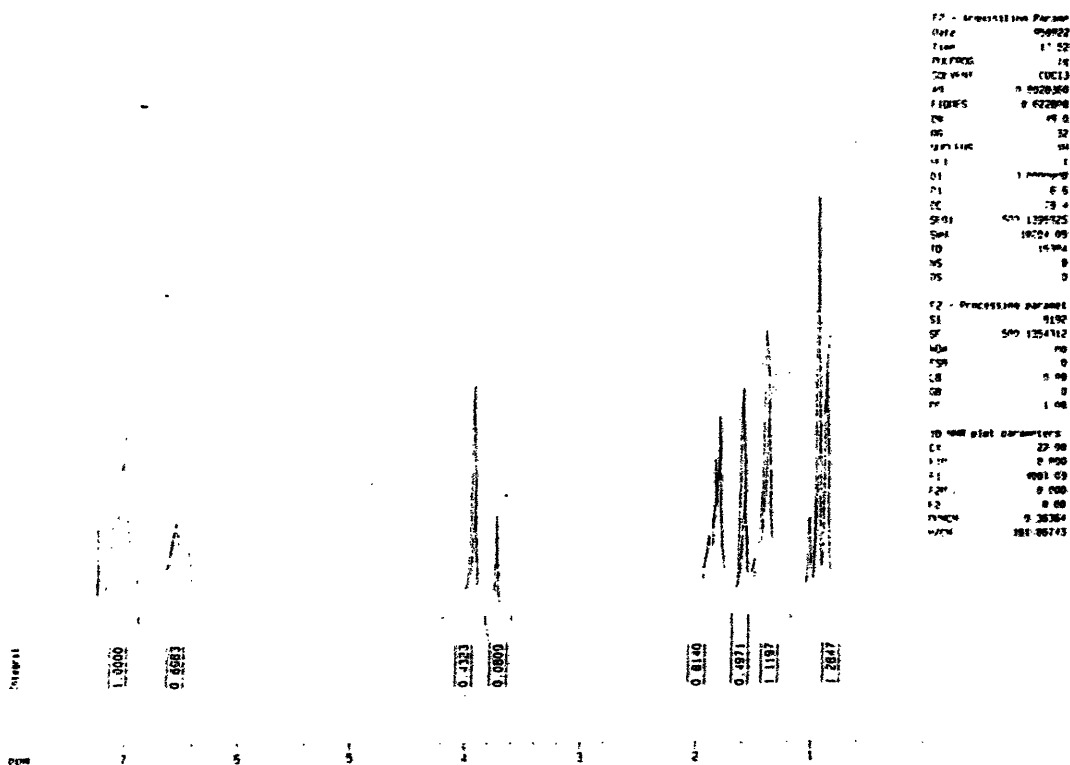


Figure 5-3 NMR spectra of 54K P(S-*b*-nBMA)

The mole fraction of styrene, x , can be calculated with Equation 5.1:

$$\frac{\text{Area (7 ppm)}}{\text{Area (4 ppm)}} = \frac{5x}{2(1-x)} \quad (5.1)$$

The mole fraction of styrene was 62% for the 54K diblock and 61% for the 210K diblock. The mole fractions were converted into weight fractions. The respective weight fractions of styrene were 55% for the 54K diblock and 53% for the 210K diblock. The composition of the 210K diblock after selective precipitation was not determined by NMR but can be estimated as 50%.

styrene based on the mass of the precipitate. The density of poly(styrene) and poly(*n*-butylmethacrylate) are both 1.05 g/mol so the weight fractions and the volume fractions are equivalent.

5.3 Neutron Scattering

The 54K and 210K P(S-*b*-*n*BMA) samples were analyzed with neutron scattering at 165°C. The results are shown in Figure 5-4. The rheology measurements of deuterated diblock copolymers P(d-S-*b*-*n*BMA)⁹ indicated that polymers below 70K did not have LCOT behavior at temperatures below 200°C. The interactions of deuterium and hydrogen are slightly different but the 54K copolymer was found to also be in the disordered state. A plot of the measured intensity versus q shows a weak maxima at $q=0.22 \text{ nm}^{-1}$ which is due to the different scattering cross sections of the styrene block and the *n*-butyl methacrylate block. This peak is predicted by Leibler for both the ordered and disordered states. The small height of this peak is indicative of a disordered diblock copolymer. Equation 2.15 shows that the radius of gyration in the disordered state is approximately 8.5 nm.

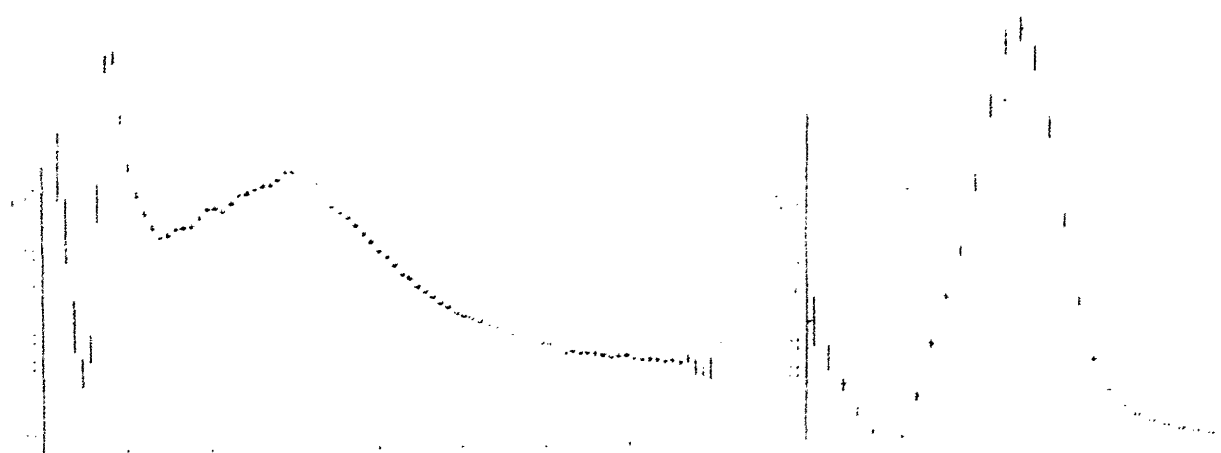


Figure 5-4. Neutron Scattering of 54K (left) and 210K (right) P(S-*b*-*n*BMA).

The SANS diffraction pattern of the 210K copolymer had a strong first order Bragg reflection. Figure 5-4 shows a peak at $q=0.10 \text{ nm}^{-1}$. Equation 2-7 shows that the periodicity of the phase separated structure is 63 nm. The strong intensity of this peak is indicative of phase separation. The periodicity of the ordered 210K copolymer should be much greater than the radius of gyration of the 54K copolymer. In addition to the higher molecular weight, each block in the ordered copolymer does not obey random walk statistics but instead is stretched to minimize interfacial area of the blocks.³⁰ The periodicity of an ordered diblock copolymer scales as $N^{2/3}$.³¹ By contrast, the radius of gyration of a disordered diblock copolymer scales as $N^{1/2}$. The periodicity of the ordered 210K copolymer is 3.7 times greater than twice the radius of gyration of the disordered 54K copolymer. If both copolymers obeyed random walk statistics, the ratio should be $(210/54)^{1/2}$ which equals 2.0.

Chapter 6

Summary and Conclusions

Three molecular weights of P(S-*b*-*n*BMA) were anionically synthesized. ¹H NMR spectroscopy and GPC chromatograms suggest that the diblock copolymers are composed of equal masses of styrene and *n*-butyl methacrylate. Homopolymer contamination is approximately 10% in these samples but selective precipitation in 60% methanol 40% benzene mixtures was successful in removing some of the polystyrene. The SANS results showed that the 54K copolymer was disordered at all measured temperatures and that the 210K copolymer was always microphase separated.

Chapter 7

Suggestions for Further Work

The difficulty of selective precipitation would be avoided if the P(S-*b*-*n*BMA) copolymers were made without homopolymer contamination. Extremely pure monomers and solvent will prevent premature termination of the polymerization. Distilling styrene with dibutylmagnesium reduces the water and alcohol content of the distillate. Trioctylaluminum is a possible desiccant for *n*-butyl methacrylate. Careful distillation of the tetrahydrofuran over sodium benzophenone is sufficient for removing impurities from the solvent.

The synthesized polymers may be useful in studying the thermodynamics and rheology of the LCOT behavior. In addition to SANS, solid state NMR is another potentially powerful technique for exploring the effects of compressibility on the thermodynamics of microphase separation. NMR has the advantage of accurately determining the effects on an atomic level. Recent experimental techniques have been developed to look at the torsional angle of carbon-carbon bonds in methacrylates and the relative orientations of the phenyl ring of polystyrene³². Applying similar techniques to P(S-*b*-*n*BMA) may elucidate the molecular origins of the compressibility effects.

Bibliography

- [1] Russell, T. P., Karis, T. E., Gallot, Y., Mayes, A. M. *Nature* **368**, 729 (1994)
- [2] Leibler, L. *Macromolecules* **13**, 1602 (1980)
- [3] Fredrickson, G. H., Helfand *J. Chem. Phys.* **87**, 697 (1987)
- [4] Ramos, A. R., Cohen, R. E. *Polym. Engineering Sci.* **17**, 639-646 (1977)
- [5] Fischer, E. W., Jung, W. G. *Makromol. Chem., Makromol. Symp.* **26** 179 (1989)
- [6] Bates, F. S., Rosedale, J. H., Blair, H.E., Russell, T.P. *Macromolecules* **22**, 2557 (1989)
- [7] Bates, F. S., Rosedale, J. H., Fredrickson, G. H. *J Chem. Phys.* **92**, 6255 (1990)
- [8] Rosedale, J. H., Bates, F. S. *Macromolecules* **23**, 2329 (1990)
- [9] Karis, T. E., Russell, T. P., Gallot, Y., Mayes, A. M. *Macromolecules* **28**, 1129 (1995)
- [10] Rempp, P., Merrill, E. *Polymer Synthesis* Heuthig&Wepf Verlag Basel (1986)
- [11] Flory, P. J. *J. Am. Chem. Soc.*, **62**, 1561 (1940)
- [12] Bates, F. S. Synthesis and characterization of cis 1-4 polyisoprene, poly *n*-butyl methacrylate and corresponding diblock copolymer. Master's thesis, Massachusetts Institute of Technology 1978
- [13] "Styrene Polymers," p30 in "Encyclopedia of Polymer Science and Engineering," Vol. 17, Mark, H.F., Bikales, N. M., Overberger, C., G., Menges, G., Eds., Wiley-Interscience, New York, 1988
- [14] Young, R.J., Lovell, P.A. *Introduction to Polymers* Chapman & Hall 1991
- [15] Flory, P. J., Orwoll, R. A., Vrij, A. *J.A.C.S.*, **86**, 3507 (1964)
- [16] Sanchez, I. C., Lacombe, R. H. *Macromolecules* **11**, 1145-1156 (1995)
- [17] Lacombe, R. H., Sanchez, I. C., *J. Phys. Chem.*, **80**, 2568 (1976)
- [18] Sanchez, I. C., Balazs, A. C., *Macromolecules*, **22**, 2325 (1989)
- [19] Hammouda, B., Bauer, B. J., *Macromolecules* **28**, 4505 (1995)
- [20] Lovessey, S. W. *Theory of Neutron Scattering from Condensed Matter* Clarendon Press, New York 1984
- [21] Dachs, H., *Neutron Diffraction* Springer-Verlag New York 1978
- [22] de Gennes, P. -G. *J. Phys.* **31**, 235 (1970)
- [23] de La Cruz, M. O., Sanchez, I. C., *Macromolecules*, **19**, 2501 (1986)
- [24] Dudowicz, J., Freed, K. F., *Macromolecules*, **23**, 1519 (1990)
- [25] Dudowicz, J., Freed, K. F., *Macromolecules*, **24**, 5112 (1991)
- [26] Dudowicz, J., Freed, K. F., *J. Chem. Phys.*, **96**, 9147 (1992)
- [27] Dudowicz, J., Freed, K. F., Lifschitz, M., *Macromolecules*, **27**, 5387 (1994)
- [28] Bidkar, U. R., Sanchez, I. C., *Macromolecules*, **28**, 3963 (1995)
- [29] Yeung, C., Desai, R. C., Shing, A., Noolandi, J. *Phys. Rev. Letters*, **12**, 1834 (1994)
- [30] Helfand, E., Wasserman, Z. R., *Macromolecules*, **9**, 879 (1976)
- [31] DiMarzio, E. A., Sanchez, I. C. *Bull. Am. Phys. Soc.*, **29**, 281 (1984)
- [32] Robyr, P., Tomaselli, M., Straka, J., Grob-Pisano, C., Suter, U. W., Meier, B. H., Ernst, R. R. *Molecular Physics* , **84** 995 (1995)

Appendix A

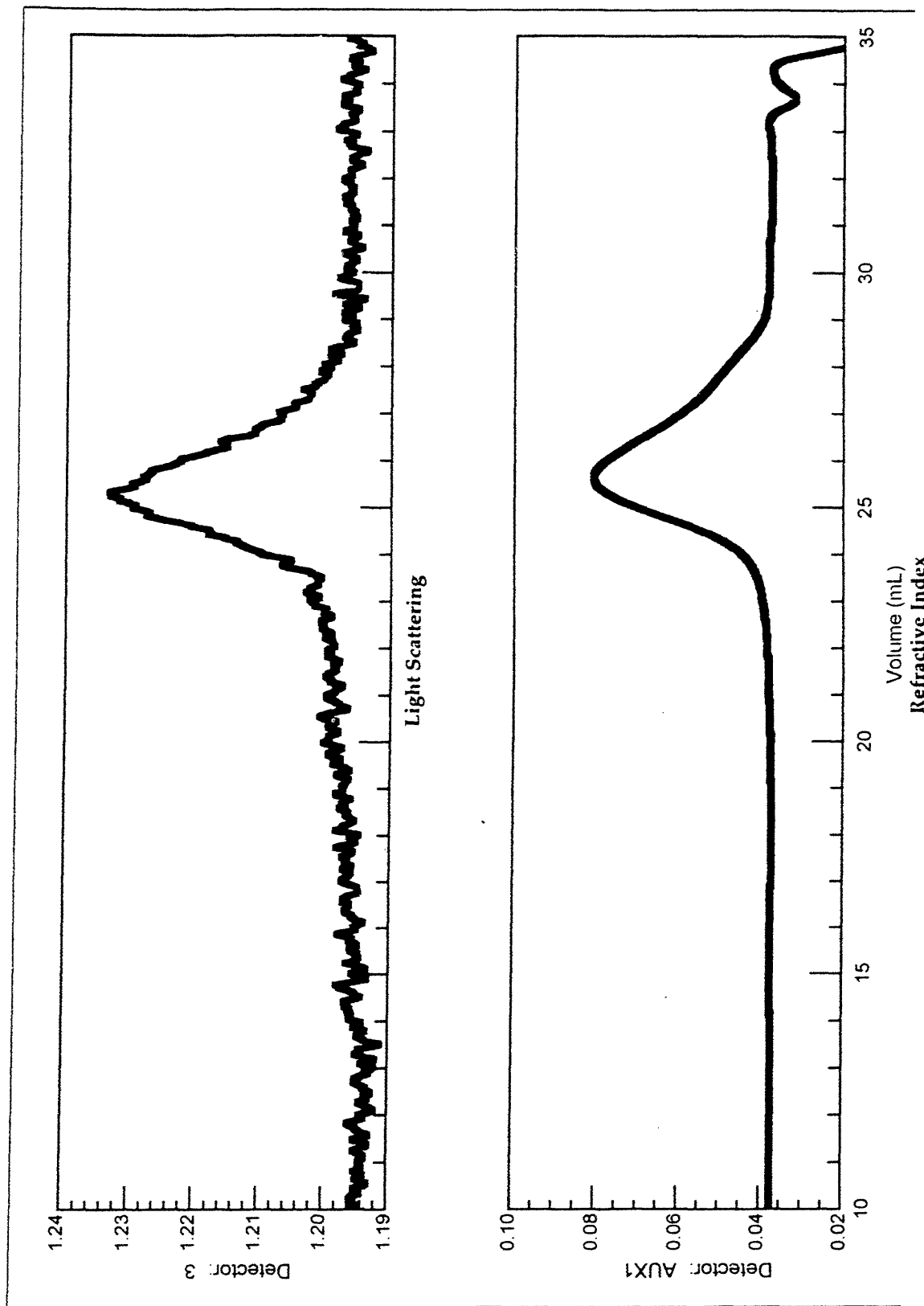


Figure A-1. GPC chromatogram. $M_n=49K$, $M_w=54K$, $PDI=1.10$

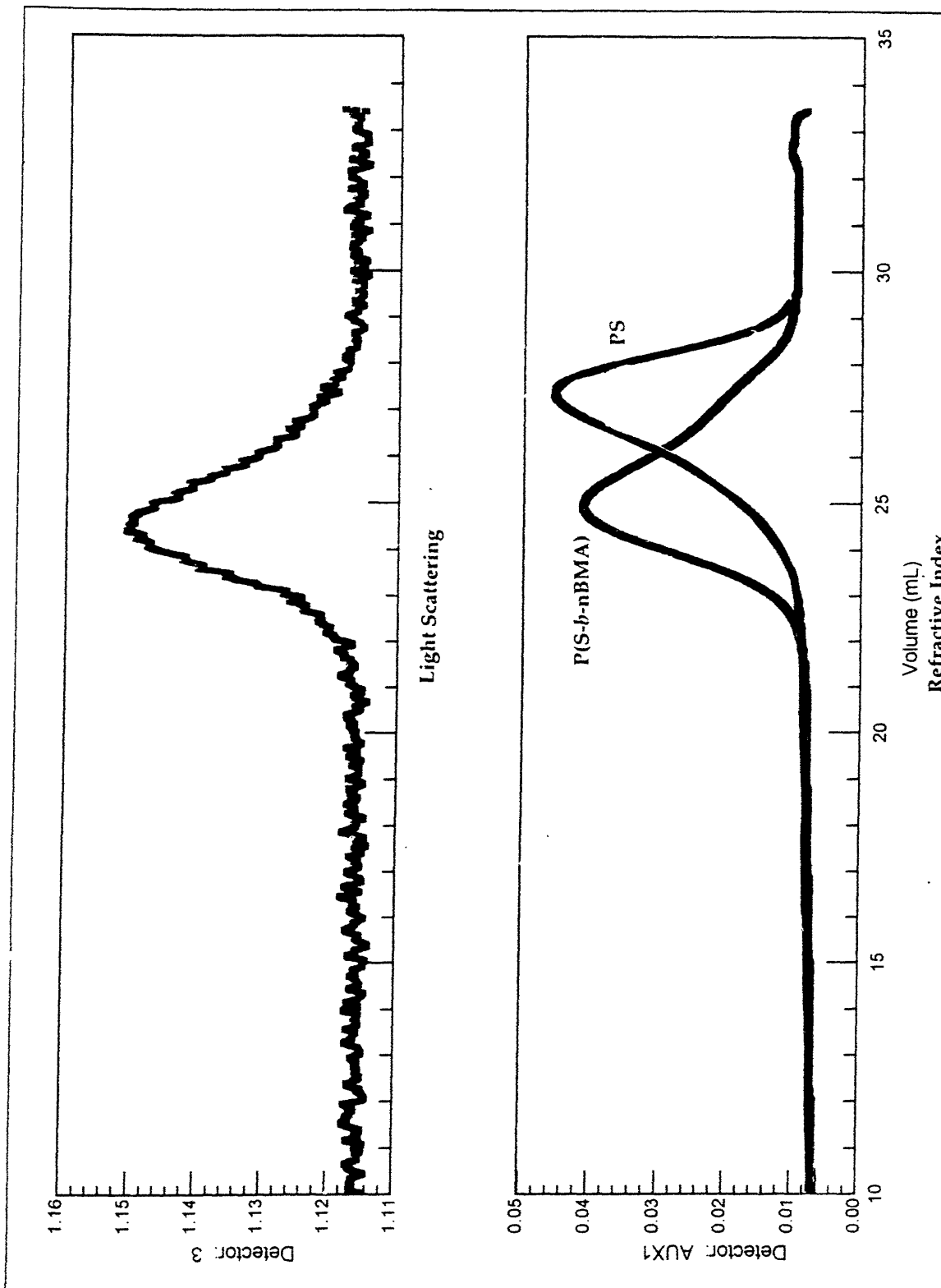


Figure A-2. GPC chromatograms. PS: $M_n=27K$, $M_w=31K$, PDI=1.12
P(S-*b*-nBMA): $M_n=66K$, $M_w=71K$, PDI=1.07

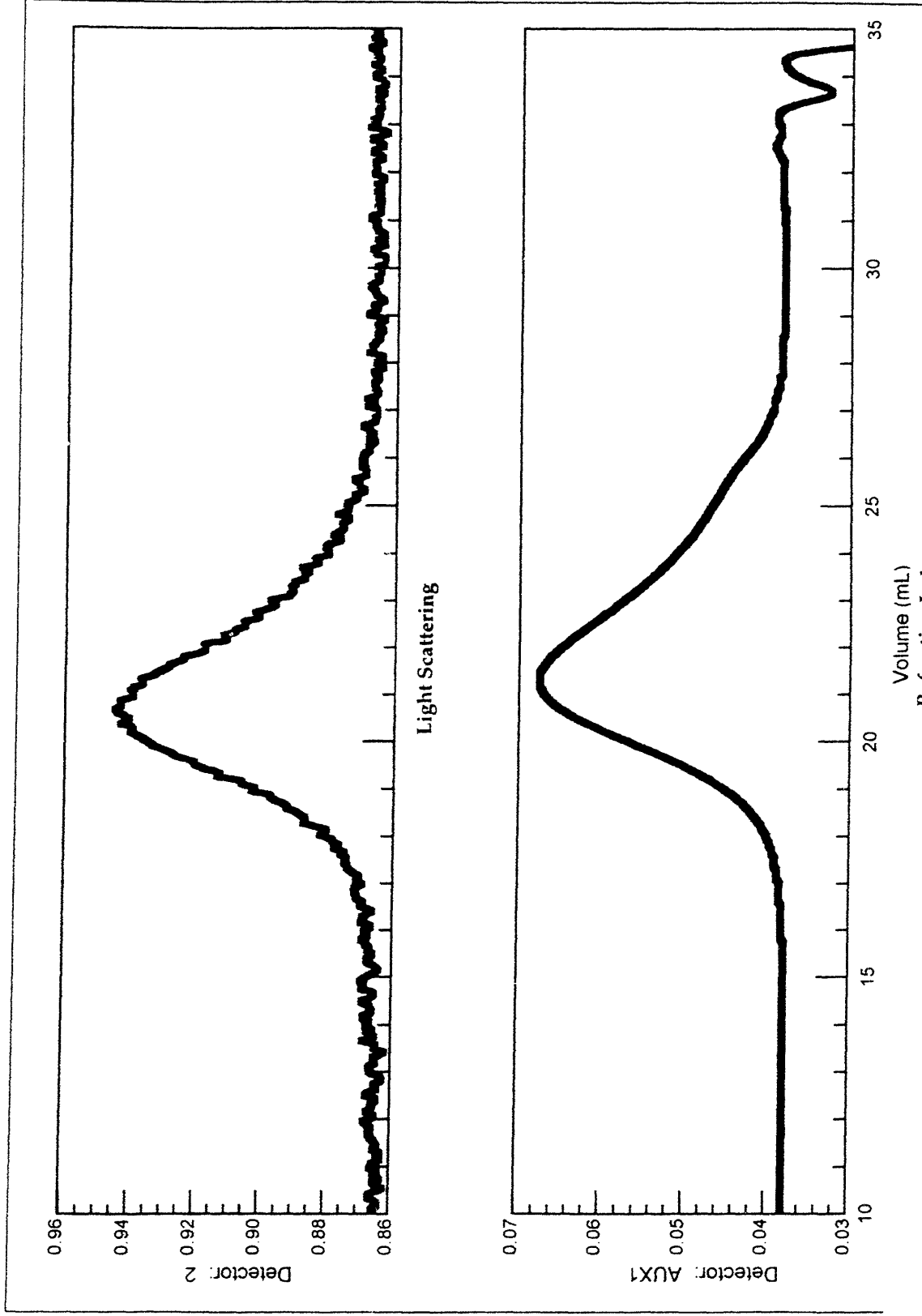


Figure A-3. GPC chromatogram. $M_n=179K$, $M_w=205K$, $PDI=1.15$

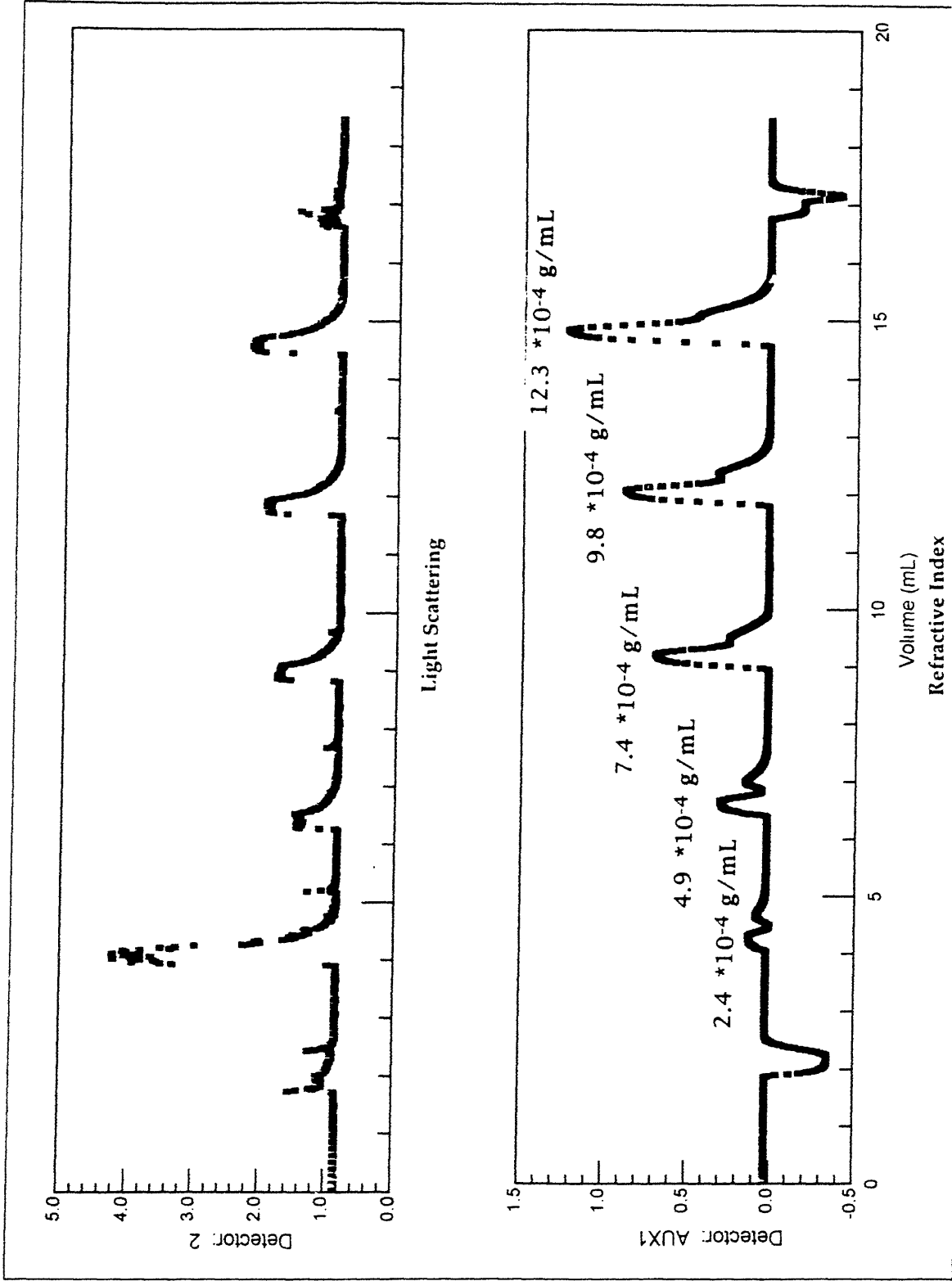


Figure A-4. Determination of dn/dc .

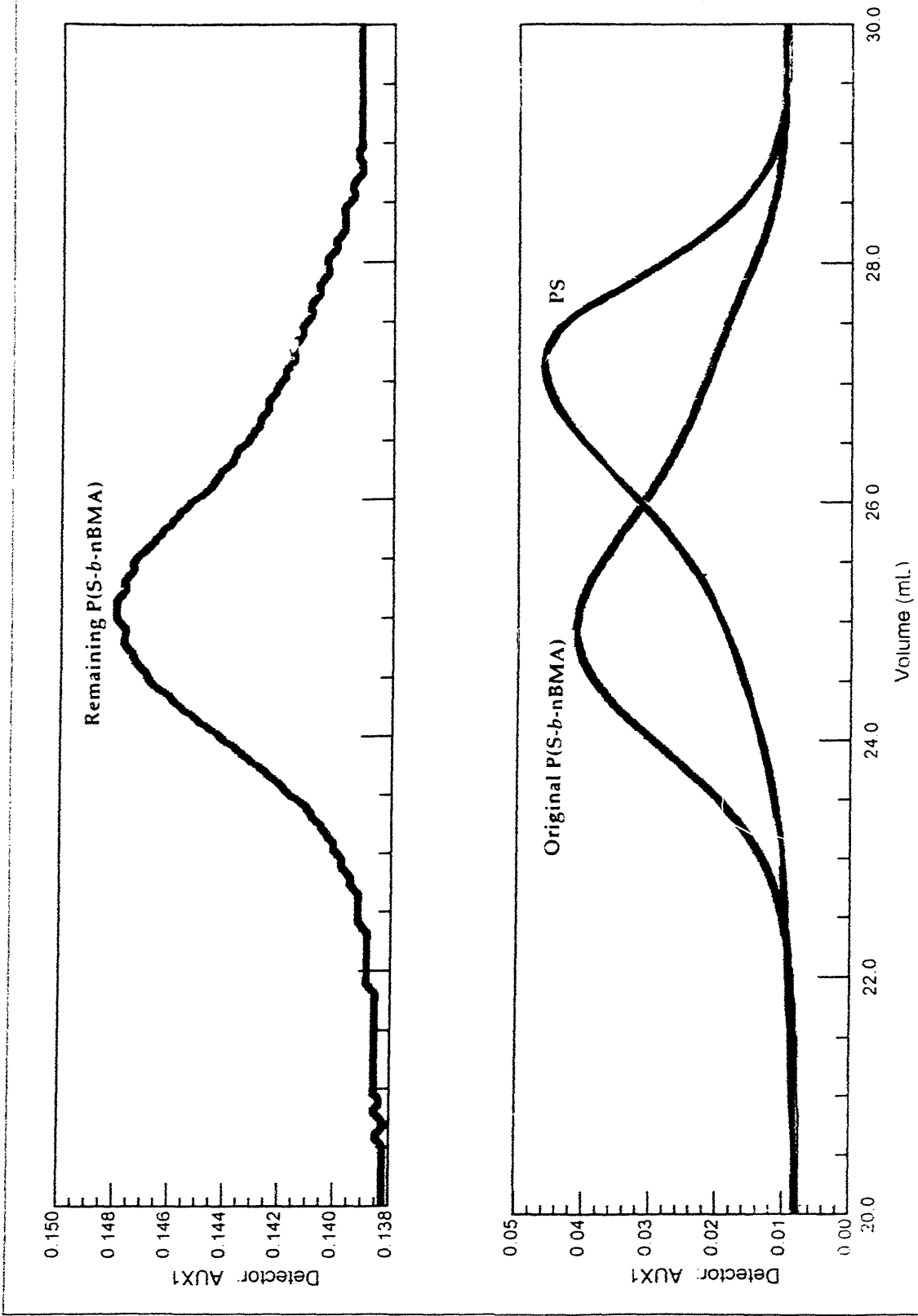


Figure A-5. Selective precipitation of 71K P(S-b-nBMA).